P Wave Delineation Using Spatially Projected Leads From Wavelet Transform Loops

R Almeida [1,2,3], JP Martínez [2,1], AP Rocha [4,3], P Laguna [2,1]

[1]Ciber - Bioingeniería, Biomateriales y nanomedicina, Zaragoza, Spain
[2]Communications and Technology Group (GTC), Aragón Institute of Engineering Research (I3A), University of Zaragoza, Zaragoza, Spain
[3] Centro de Matemática, Universidade do Porto (CMUP), Porto, Portugal
[4] Departamento de Matemática, Faculdade de Ciências, Universidade do Porto, Porto, Portugal

Abstract

A previously proposed automatic delineation strategy for multilead (ML) location of wave boundaries is now extended to P wave boundaries. The method obtains a transformed lead by projecting the wavelet transform spatial loop into a direction that optimizes the SNR. The performance was compared with single lead delineation (SL) and with the global marks obtained by post-processing rules (SLR) calculating the Sensitivity, mean and standard deviation $[S(\%),\ m \pm s$ *(ms)]* *respectively for onset| end location errors. Validation is performed over CSE database files obtaining, using 3D loops* $[100, -10.2 \pm 15.0] \mid [100, 7.8 \pm 14.2]$*, and using 2D loops* $[96, -2.4 \pm 7.4] \mid [96, 5.9 \pm 7.0]$*. SLR achieved* $[85, 2.1 \pm 5.6] \mid [89, 1.8 \pm 6.7]$*, with SL producing always higher* s *values in one or both boundaries. We conclude that ML strategy is appropriate for P wave delineation, with higher* S *that SLR, and 2D loops are sufficient, allowing a more efficient processing when compared to SLR.*

1. Introduction

According to the dipolar hypothesis, the electrical activity of the heart can be approximated by a time-variant electrical dipole, called the *electrical heart vector* (EHV). Thus, the voltage measured at a given lead would be the projection of the EHV into the unitary vector defined by the lead axis [1]. Choosing a particular lead for ECG delineation determines a point of view over the cardiac phenomena and different latencies on the waves's onsets and ends are found in different leads. Nevertheless, the onset and end of the cardiac electric phenomena are indeed unique, and therefore a global lead-independent feature.Thus combining adequately the information provided by multiple leads is essential for the correct location of lead-independent waves' boundaries. To achieve this goal, methodologies based on several leads should be used.

We have previously proposed a wavelet transform (WT) based single-lead ECG delineation system (SL) [2] which includes post-processing decision rules (SLR) to deal with multilead files, by constructing global marks from the single lead based sets of locations. Nevertheless SLR does not take advantage of the leads' spatial dependency and it requires a large number of leads to achieve stable marks. To cope with this, the SL system was enhanced regarding the QRS complex and T wave boundaries by a strategy that uses a transformed lead obtained from vectocardiographic (VCG) loops. The WT spatial loop is projected into a direction that optimizes the SNR and so the delineation. SL delineation is then applied to the synthesized lead, providing unique locations for wave boundaries. In this work the multilead methodology (ML) was extended to the P wave boundaries and validated over standard databases.

2. Multilead delineation strategy

The ML delineation system was proposed in [3], implemented and validated regarding QRS complex and T wave boundaries. The method considers the VCG loops given by any three simultaneous orthogonal leads $\mathbf{s}[n] = [x(n), y(n), z(n)]^T$ to obtain the respective WT *loop* $\mathbf{w}_m[n]$, for a given scale $2^m, m \in \mathbb{N}$. The WT system used is such that the WT at scale 2^m, $w_{x,m}[n]$, is proportional to the derivative of the filtered version of the signal $x[n]$ with a smoothing impulse response at scale 2^m. Thus, ECG wave peaks correspond to zero crossings in the WT, ECG maximum slopes correspond to WT's maxima and minima and the loop $\mathbf{w}_m[n]$ is proportional to the VCG derivative, describing the velocity of evolution of the EHV. The main direction $\mathbf{u} = [u_{\mathrm{X}}, u_{\mathrm{Y}}, u_{\mathrm{Z}}]^T$ of EHV variations in a scale 2^m is given by the director vector of the best straight linear fit to all points in $\mathbf{w}_m[n]$ and it defines the ECG lead maximizing the local SNR, and thus,

the most appropriate for boundary delineation. Considering WT loops in a 2D plane instead of in a 3D space is also possible, allowing to apply this methodology to any two ECG orthogonal leads. The strategy is similar to the one for T wave boundaries, with the specificities described in the following algorithm.

For each beat k:

INITIALIZATION

$a_0)$ Let's be $n_{\mathrm{QRS,o}}(\mathrm{k})$ the ML based QRS onset location for beat k and $n_{\mathrm{last}}(\mathrm{k}-1)$ the last annotation on the beat $\mathrm{k}-1$ (typically a T wave end). The initial P wave search window $\mathrm{P}^{(1)} = \mathrm{P}_{\mathrm{o}}^{(1)} = \mathrm{P}_{\mathrm{e}}^{(1)}$ is defined as:
$[Max\left[n_{\mathrm{QRS,o}}\left(\mathrm{k}\right) - 0.34s; n_{\mathrm{last}}(\mathrm{k}-1)\right]; n_{\mathrm{QRS,o}}(\mathrm{k}) - 0.1\mathrm{s}];$
$b_0)$ the initial main direction of EHV variations $\mathbf{u}^{(1)}$ is estimated as the best line fit in total least squares (TLS) sense to the WT loop $\mathbf{w}_4[n], n \in \mathrm{P}^{(1)}$;
$c_0)$ the loop $\mathbf{w}_4\left[n\right], n \in [n_{\mathrm{QRS}}\left(\mathrm{k}-1\right),\ n_{\mathrm{QRS}}(\mathrm{k}+1)]$, for $n_{\mathrm{QRS}}(\mathrm{k})$ the median of SL derived locations for the QRS complex in the k^{th} beat, is projected over $u^{(1)}$ to construct the new derived WT signal $w_{d,4}^{(1)}[n]$;
$d_0)$ SL delineation over $w_{d,4}^{(1)}[n]$ allows to locate $n_{\mathrm{P,o}}^{(1)}$ and $n_{\mathrm{P,e}}^{(1)}$, the boundaries positions at step 1.

ITERATION - STEP (i); separately for each boundary:
a) the search window $\mathrm{P}^{(\mathrm{i})}$ is updated attending to the boundary location provided by the previous step $(\mathrm{i}-1)$, separately for onset | end:

$$\mathrm{P}_{\mathrm{o}}^{(\mathrm{i})} = \left[n_{\mathrm{P,o}}^{(\mathrm{i}-1)}(\mathrm{k}) - 4\mathrm{s}_{\mathrm{CSE}}(\mathrm{P_{on}});\ n_{\mathrm{P,f}}^{(\mathrm{i}-1)}(\mathrm{k})\right];$$
$$\mathrm{P}_{\mathrm{e}}^{(\mathrm{i})} = \left[n_{\mathrm{P,l}}^{(\mathrm{i}-1)}(\mathrm{k});\ n_{\mathrm{P,e}}^{(\mathrm{i}-1)}(\mathrm{k}) + 4\mathrm{s}_{\mathrm{CSE}}(\mathrm{P_{end}})\right];$$

where $n_{\mathrm{P,o}}^{(\mathrm{i}-1)}(\mathrm{k})|\mathrm{n}_{\mathrm{P,e}}^{(\mathrm{i}-1)}(\mathrm{k})$ is the P *onset*|*end* position, according to iteration $(\mathrm{i}-1)$, $n_{\mathrm{P,f}}^{(\mathrm{i}-1)}(\mathrm{k})|\mathrm{n}_{\mathrm{P,l}}^{(\mathrm{i}-1)}(\mathrm{k})$ is the location of the *first*|*last* significant maximum modulus, associated to the P wave in $w_{d,4}^{(\mathrm{i}-1)}[n]$ and $s_{\mathrm{CSE}}(\mathrm{P}on) = 5.1$ ms $s_{\mathrm{CSE}}(\mathrm{P}end) = 6.35$ ms are the tolerance values given in [4] for P wave onset | end location error;
b) the main direction of EHV variations $\mathbf{u^{(i)}}$ is estimated as the TLS best line fit to $\mathbf{w}_4[n], n \in P_{\mathrm{o}}^{(\mathrm{i})}|n \in P_{\mathrm{e}}^{(\mathrm{i})}$;
c) the new derived WT signal $w_{d,4}^{(\mathrm{i})}[n]$ is constructed by projecting the loop $\mathbf{w}_4[n], n \in [n_{\mathrm{QRS}}(\mathrm{k}-1)\ ,\ n_{\mathrm{QRS}}(\mathrm{k}+1)]$;
d) IF $n_{\mathrm{P,f}}^{(\mathrm{i})}|n_{\mathrm{P,l}}^{(\mathrm{i})}$ has lower amplitude than $n_{\mathrm{P,f}}^{(\mathrm{i}-1)}|n_{\mathrm{P,l}}^{(\mathrm{i}-1)}$, OR no significant maximum of $w_{d,4}^{(\mathrm{i})}[n]$ was found;
THEN it is considered that the lead constructed at step (i) is less fitted for P *onset*|*end* location than the constructed in the step $(\mathrm{i}-1)$ and $n_{\mathrm{P,o}}^{(\mathrm{i}-1)}$ or $n_{\mathrm{P,e}}^{(\mathrm{i}-1)}$ (found in the previous step) is adopted as ML mark; STOP;
ELSE SL delineation of the boundary is performed over $w_{d,4}^{(\mathrm{i})}[n]$ to find $n_{\mathrm{P,o}}^{(\mathrm{i})}$ or $n_{\mathrm{P,e}}^{(\mathrm{i})}$ updated marks;
e) IF the *first*|*last* significant maximum of $w_{d,4}^{(\mathrm{i})}[n]$ found is equal to the one found in a previous step THEN $n_{\mathrm{P,o}}^{(\mathrm{i})}|n_{\mathrm{P,e}}^{(\mathrm{i})}$ is adopted as ML mark; STOP;
ELSE REPEAT from a).

The ML P wave delineation is illustrated for the wave end in Figure 1.

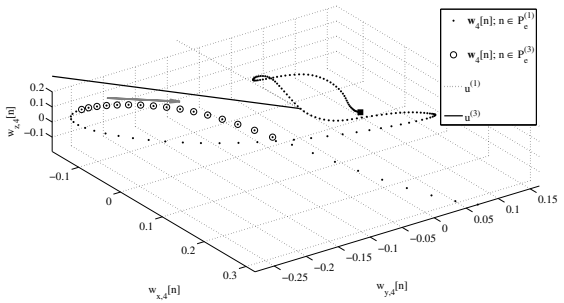

(a)WT loop and the direction of the best line fit at the initial and final step.

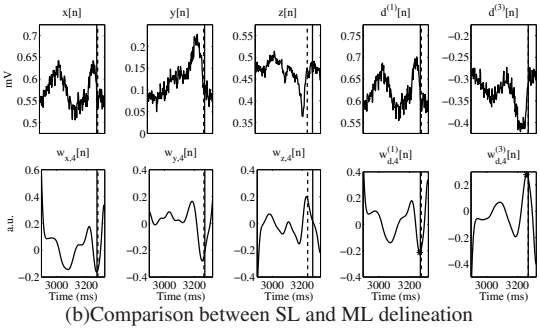

(b)Comparison between SL and ML delineation

Figure 1. Example of P wave onset delineation. In a) the big square stands for the first $\mathrm{P}^{(1)}$ sample, arrow indicates time direction; in b) vertical dashed lines stand for the mark found in the respective lead, vertical solid lines stand for referee marks, the stars stand for the first significant maximum modulus in the constructed lead.

3. Data and validation

Two standard databases with annotated reference beats were considered for validation purposes, by comparing the marks found with the provided referee marks.

The CSE multilead measurement database (CSEDB [5], 15 leads at 500 Hz) includes median manual P wave annotations for 26 onsets and 27 ends. Two different VCG systems were considered for ML delineation: lead set **F**, defined by recorded orthogonal Frank leads (X,Y,Z) and lead set **D**, defined by the synthesised orthogonal leads (X,Y,Z) from the 12-lead system, by using the coefficients provided by the inverse *Dower Matrix* [6]. Combinations of each 2 orthogonal lead pairs were also considered both using lead set **F** and lead set **D**, defining lead sets: $\mathbf{F_{XY}}$, $\mathbf{F_{XZ}}$, $\mathbf{F_{YZ}}$, $\mathbf{D_{XY}}$,$\mathbf{D_{XZ4}}$, $\mathbf{D_{YZ}}$. For comparison purposes SL delineation [2] was applied over each of the 15 recorded leads and global SLR marks obtained by ordering the 12 sets of annotations corresponding to the standard lead system and selecting as the *onset*|*end* as the *first*|*last* annotation whose 3 nearest neighbours lay within a 4 ms interval [7].

The QT database (QTDB [8], 2 leads at 250 Hz) includes manual annotations for 2983 P wave onsets and ends. Since QTDB only includes 2 leads, ML was applied using loops in the 2D plane. Subgroups of files regarding the orthogonality of the leads were considered: **QTDB1** , includes the 7 records with orthogonal leads from the 12-lead standard system, in which the ML delineation can be applied directly using a 2D approach; **QTDB2** includes 57 records with no identified leads, here assumed to be orthogonal and treated as the ones in **QTDB1**; finally **QTDB3** includes the 34 records with no orthogonal and no parallel leads, which were orthogonalized by constructing a new ECG lead orthogonal to one of the provided leads. The SL delineation was applied to each of the 2 leads and a combined mark was obtained by choosing for each fiducial point the location on the lead with less error (**best mark**). Notice that the **best mark** approach cannot be applied when no reference marks exist. It is used as a way to compare the SL annotation sets with the manual annotations performed having in view the two leads.

The *detection* performance was evaluated calculating the *Sensitivity*, $S = 100\frac{TP}{TP+FN}$, where *TP* is the number of true positive detections and *FN* stands for the number of false negative detections. The delineation error (ε) was taken as the *automatically detected boundary minus the respective referee mark*. In CSEDB were evaluated the mean (m_ε) and standard deviation (s_ε) of ε across files, while in QTDB, since several beats are annotated per file, the standard deviation of the error ε was first calculated across beats for each file and then averaged across records $(\bar{s}_\varepsilon)$.

4. Results and discussion

The results obtained over CSEDB files are presented in Table 1 (ML over Frank or Dower lead set and SLR over the 12 standard leads) and in Figure 2 (same as before plus 2D subsets of leads, and SL over each lead available). The results over the files of QTDB are presented in Table 2 for each subgroup and for all files.

Globally a better performance was achieved for P wave end than for P wave onset. The lead set ***F*** allowed to locate the boundaries for all annotated P waves in CSEDB, with an error standard deviation $s \leq 15$ ms for both boundaries. The best performance with SL for P wave end is achieved over lead X $[100\%, 2.2 \pm 9.8$ ms] but with poor performance for P wave onset $[100\%, -6.5 \pm 31.1$ ms]. As a matter of fact, SL always performs worse that ML in one or both the boundaries for all cases. In spite of lower m and s values atained by SLR, they are referred to a lower number of TP, as $S < 90\%$ for both bondaries.

With respect to 2D approach, using just leads X and Y produces a small performance loss with respect to the best 3D approach, both using ***F*** $[100\%, -6.5 \pm 18.0$ ms $\mid 96\%, 3.1 \pm 15.8$ms] and ***D*** $[96\%, -2.4 \pm 7.4$ ms $\mid 96\%, 5.9 \pm 7.0$ ms]. In QTDB ML allowed an S equal or higher than the best of the 2 SL results in both boundaries, except for files with orthogonalized leads, for which lead 2 performs better. The locations found are at least as much stable as the ones provided by the best of the SL results (s values lower or similar). According to the results in both databases, there exists a pair of 2 orthogonal leads apparently sufficient to P wave boundaries location. This can indicate that the EHV changes on the P wave boundaries are mainly along a single plane, not requiring a 3D description. At the CSE database D12 is the plane providing the best performance.

5. Concluding remarks

The results obtained allow us to conclude that the proposed multilead strategy is appropriated for P wave delineation, with an higher Sensitivity than using post processing rules to construct global marks from single annotations. Moreover using 2D loops, in spite of some performance loss, still performs better than using single lead.

Acknowledgements

This work was partially supported by project TEC2007-68076-c02-02 from MCyT and FEDER, Grupo Consolidado GTC from DGA T:30. CIBER-BBN is an initiative funded by the VI National R&D&i Plan 2008-2011, Iniciativa Ingenio 2010, Consolider Program, CIBER Actions and financed by the Instituto de Salud Carlos III with assistance from the European Regional Development Fund. CMUP is financed by FCT, Portugal, through the programmes POCTI and POCI 2010, with national and European Community Structural Funds.

References

[1] Malmivuo J, Plonsey R. Bioelectromagnetism - Principles and Applications of Bioelectric and Biomagnetic Fields. Oxford University Press, 1995.

[2] Martínez JP, Almeida R, Olmos S, Rocha AP, Laguna P. Wavelet-based ECG delineator: evaluation on standard databases. IEEE Transactions on Biomedical Engineering 2004;51:570–581.

[3] Almeida R, Martínez JP, Rocha AP, Laguna P. Multilead ECG delineation using spatially projected leads from wavelet transform loops. IEEE transactions on biomedical engineering Aug 2009;56(8):1996–2005.

[4] The CSE Working Party. Recomendations for measurement standards in quantitative electrocardiography. Eur Heart J 1985;6:815–825.

[5] Willems JL, Arnaud P, van Bemmel JH, Bourdillon PJ, Degani R, Denis B, Graham I, M. HF, Macfarlane PW, Mazzocca G, et al. A reference data base for multilead electrocardiographic computer measurement programs. J Am Coll Cardiol 1987;10(6):1313–1321.

Table 1. P wave boundaries delineation results in CSEDB: True positive detections (TP) out of referee beats (#), Sensitivity ($S\%$), mean and standard deviation ($m \pm s$, ms)

	P onset			P end		
	ML F	ML D	SLR	ML F	ML D	SLR
$TP/\#$ $(S,\%)$	$26/26(100)$	$25/26(96)$	$22/26(85)$	$27/27(100)$	$25/27(92)$	$24/27(89)$
$m \pm s$, ms	-10.2 ± 15.0	-4.9 ± 14.6	2.2 ± 5.6	7.8 ± 14.2	4.0 ± 10.8	1.8 ± 6.7

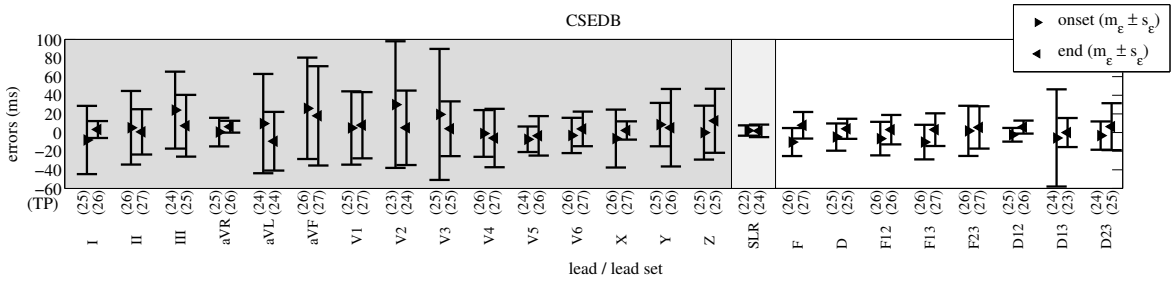

Figure 2. P wave boundaries delineation results in CSEDB:comparison between SL, SLR and ML.

Table 2. P wave boundaries delineation results in QTDB.

(a)P wave onset

		ML	lead 1 SL	lead 2 SL	best mark
QTDB1	TP / 167 $(S,\%)$	166 (99)	165 (99)	128 (77)	167 (100)
(orthogonal leads: 7 files)	$m_\varepsilon \pm \bar{s}_\varepsilon$, ms	2.0 ± 23.2	-9.1 ± 28.0	-9.8 ± 25.0	-3.9 ± 17.8
QTDB2	TP / 1684 $(S,\%)$	1564 (93)	1566 (93)	1556 (92)	1646 (98)
(unknown leads: 57 files)	$m_\varepsilon \pm \bar{s}_\varepsilon$, ms	6.6 ± 22.8	5.5 ± 25.6	-2.8 ± 24.1	7.4 ± 14.6
QTDB3	TP / 1132 $(S,\%)$	1082 (96)	1070 (95)	1119 (99)	1130 (100)
(orthogonalized leads: 34 files)	$m_\varepsilon \pm \bar{s}_\varepsilon$, ms	4.5 ± 25.0	2.6 ± 28.4	-3.8 ± 27.9	4.5 ± 15.0
all	TP / 2983 $(S,\%)$	2812 (94)	2803 (94)	2802 (94)	2947 (99)
(98 files)	$m_\varepsilon \pm \bar{s}_\varepsilon$, ms	5.5 ± 23.6	3.5 ± 26.8	-3.6 ± 25.5	5.6 ± 14.9

(b)P wave end

		ML	lead 1 SL	lead 2 SL	best mark
QTDB1	TP / 167	166 (99)	165 (99)	128 (77)	167 (109)
(orthogonal leads: 7 files)	$m_\varepsilon \pm \bar{s}_\varepsilon$, ms	0.6 ± 13.6	-0.7 ± 13.0	-9.3 ± 19.3	0 ± 17.8
QTDB2	TP / 1684	1564 (93)	1566 (93)	1556 (92)	1646 (98)
(unknown leads: 57 files)	$m_\varepsilon \pm \bar{s}_\varepsilon$, ms	5.4 ± 18.1	9.8 ± 18.6	8.5 ± 24.6	7.6 ± 14.6
QTDB3	TP / 1132	1082 (96)	1070 (95)	1119 (99)	1130 (100)
(orthogonalized leads: 34 files)	$m_\varepsilon \pm \bar{s}_\varepsilon$, ms	1.4 ± 15.4	5.5 ± 20.4	1.9 ± 17.2	3.1 ± 10.8
all	TP / 2983	2812 (94)	2801 (94)	2803 (94)	2943 (99)
(98 files)	$m_\varepsilon \pm \bar{s}_\varepsilon$, ms	3.7 ± 16.9	7.6 ± 18.8	5.0 ± 21.6	5.6 ± 13.0

[6] Dower GE. The ECGD: a derivation of the ECG from VCG leads. J Electrocardiol 1984;17(2):189–91.

[7] Laguna P, Jané R, Caminal P. Automatic detection of wave boundaries in multilead ECG signals: Validation with the CSE database. Comput Biomed Res February 1994; 27(1):45–60.

[8] Laguna P, Mark RG, Goldberger A, Moody GB. A database for evaluation of algorithms for measurement of QT and other waveform intervals in the ECG. In Computers in Cardiology 1997. 1997; 673–676.

Address for correspondence:

Rute Almeida
Dpto. de Ingeniería Electrónica y Comunicaciones
Edíficio I+D+i, Mariano Esquillor, s/n, 50018 Zaragoza, España
rbalmeid@unizar.es